AAPM 2021
JULY 25–29 | VIRTUAL
63RD ANNUAL MEETING & EXHIBITION

# Cherenkov Imaging for TSE patients using cameras from multiple angles

Timothy C. Zhe[1], Yihong Ong[1], Wqeili Zhong[1], Hongjing Sun[1], Mario Gallardo[1], Petr Bruza[2], Tianshun Miao[3], Andreea Dimofte[1], Amit Maity[1], John P. Plastaras[1], Ima Payder[1], Lei Dong[1], and Brian W. Pogue[2]

[1]Perelman Center for Advanced Medicine, Univ of Pennsylvania, Philadelphia, PA, USA, [2] Thayer School of Engineering, Dartmouth College, Hanover, NH, USA, [3]Department of Radiology, School of Medicine, Yale University, New Haven, CT, USA

## INTRODUCTION

Total skin electron Therapy (TSET) has proven to be one of the most effective treatments for cutaneous T-cell lymphoma (mycosis fungoides) [1]. Cherenkov imaging has been used to quantify the dose distribution for TSE patients [2]. However, there are several deficiencies of the previous Cherenkov imaging setup for TSET: (1) The Cherenkov camera is mounted on a tripod and its position is not reproducible for day-to-day Cherenkov imaging. (2) There is only one camera looking at Cherenkov imaging from the front side and the Cherenkov emission from the side is either under- or over-estimated due to oblique emission of Cherenkov photons. Thus, we have introduced a new setup that uses 3 wall-mounted Cherenkov imaging cameras for simultaneously Cherenkov imaging of TSET patients.

## AIM

The purpose of this study is to evaluate the performance of a new generation multi-angle Cherenkov imaging cameras and 3D structure cameras for Cherenkov imaging of TSET patients .

## METHOD

Figure 1 shows the front Cherenkov camera (Fig. 1a) and the two side Cherenkov cameras (Fig. 1 b&d) as well as the front of the TSE stand (Fig. 1c). A 6 MeV HDTSe beam from a Varian Truebeam Linac is used for TSET treatment at SSD = 500 cm in a TSET stand with a 3-mm thick scattering sheet using a Stanford technique [3]. The Cherenkov-to-dose conversions were measured in a cube with diode detectors attached to 3 sides (Fig.1) and a cylinder (not shown) at the same location. In addition to Cherenkov-to-dose measurements in a cube and a cylinder, the flood image of each camera was taken with a uniform light source. Finally, the Cherenkov images were taken in a patient and converted to dose after correction with flood images and renormalized to dose at umbilicus point using OSLDs.

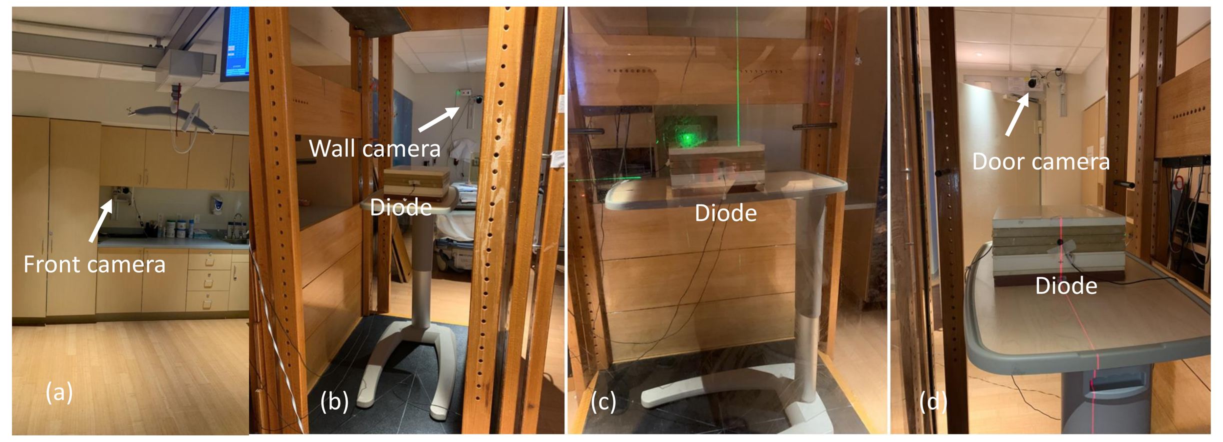


*Figure 1: Picture of (a) front mounting Cherenkov camera located at ~ 700 cm from the cube; (b) wall mount Cherenkov camera at ~250 cm from the cube and side view of a cube phantom; (c) Front view of TSE stand with a cube phantom; (d) door mount Cherenkov camera at ~ 250 cm from the cube and side view of a cube phantom.*

## RESULTS

Figure 2 shows the flood images of the three cameras: camera at the door (cam0), camera in the front (cam1), and camera at the wall (cam2). This is used to correct the camera sensitivity variation in 2D. The ranges of variation along the vertical direction through the center are 0.55 – 1, 0.83 – 1, and 0.55 – 1 for cam0, cam1, cam2, respectively; and are 0.78 – 1, 0.93 – 1, and 0.6 – 1 along the horizontal direction through the center (600, 960) for cam0, cam1, cam2, respectively. Figure 3 shows the raw Cherenkov images for 1000MU of the cube phantom (Fig. 1) in the upper row and the flood-corrected Cherenkov imaging in the lower row. The flood correction is performed by dividing the raw Cherenkov by the corresponding flood imaging in Fig. 2. The ratios of dose on the sides to that facing the radiation are 0.24 and 0.25 for the door and wall side, respectively. Figure 4 shows the linear relationship between the raw Cherenkov intensity and the dose (Fig. 4a) at the location of the diode detectors (see Fig. 1) using data obtained for MU = 1000 and 5000. Similar linear relationship can be obtained between the flood-corrected Cherenkov intensity and the dose (Fig. 4b). Notice that the slope for cam0 and cam2 are very similar, 0.0080 and 0.0084, while that for cam1 are 16% higher, 0.0094. Figure 5 shows the raw (upper row) and flood-corrected (bottom row) Cherenkov images for the cylinder. The ratios of dose on the sides to that facing the radiation are 0.39 and 0.42 for the door and the wall side, respectively, based on ratio of flood-corrected Cherenkov intensity and its relationship to dose (Fig. 4). Figure 6 shows the 6 postures (AP, LPO, RPO; PA, LAO, RAO) of a patient undergoing TSET. Figure 7 shows the raw Cherenkov images for AP position for the three cameras. Figure 8 shows the Cherenkov-converted dose map for all postures from cam1.

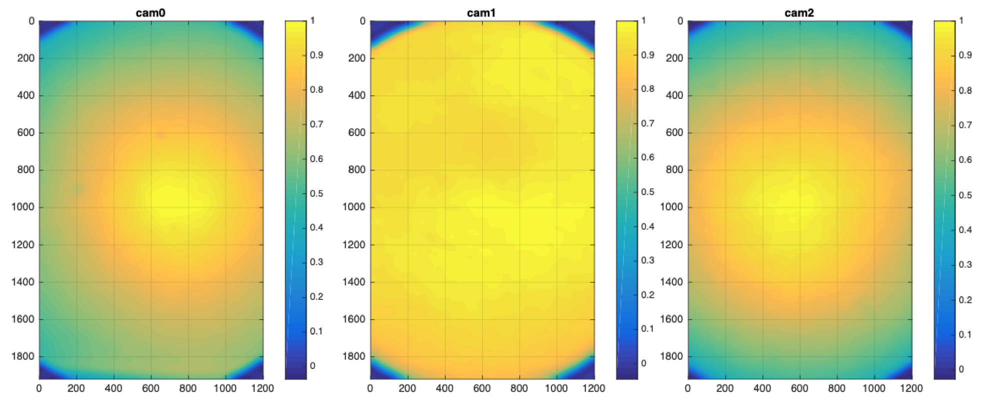


*Figure 2: Flood image (normalized to 1 at max point) for Cherenkov cameras at door (cam0), front (cam1), and wall (cam2).*

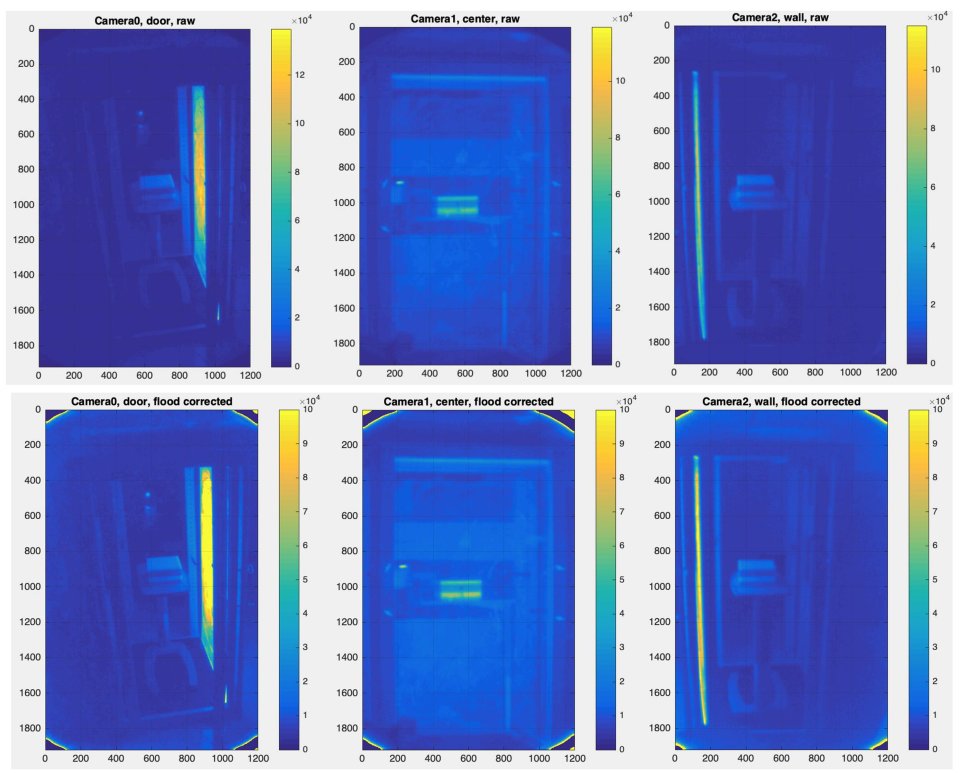

*Figure 3: Cherenkov images of a cube phantom for 1000 MU dose irradiation using a 90-degree gantry 6 MeV HDTSe beam in TSET position (500 cm SSD). Upper rows are the raw Cherenkov images for the three cameras (door, center, and wall). Bottom rows are the flood-corrected Cherenkov images (door, center, and wall).*

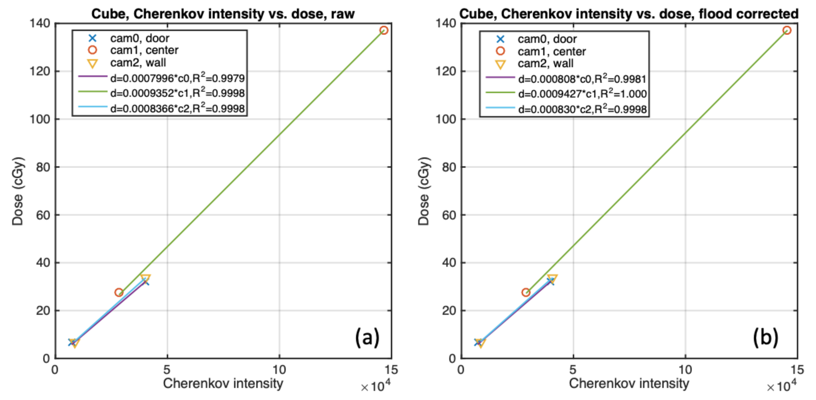


*Figure 4: Linear relationship between Dose and Cherenkov intensities for the three cameras for the cube phantom (Fig. 3) using 1000 and 5000 MU*

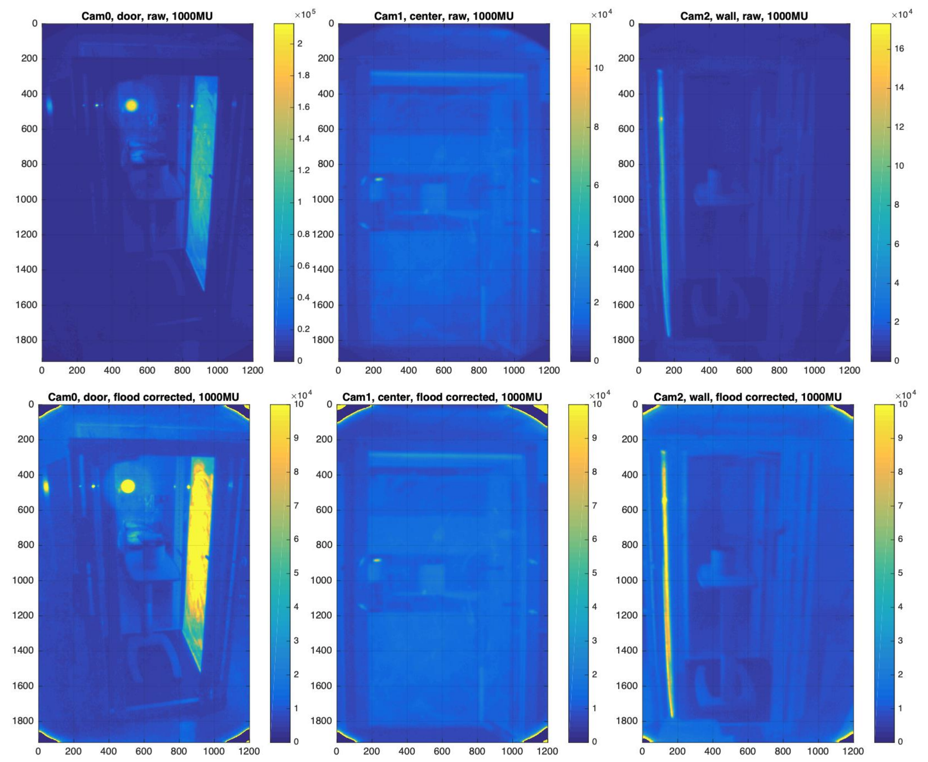

*Figure 5: Cherenkov images of a cylinder phantom for 1000 MU dose irradiation using a 90-degree gantry 6 MeV HDTSe beam in TSET position (500 cm SSD). Upper rows are the raw Cherenkov images for the three cameras (door, center, and wall). Bottom rows are the flood-corrected Cherenkov images (door, center, and wall).*


*Figure 6: The 6 postures of the patient (#38) undergoing TSET based on 3D structure scan.*

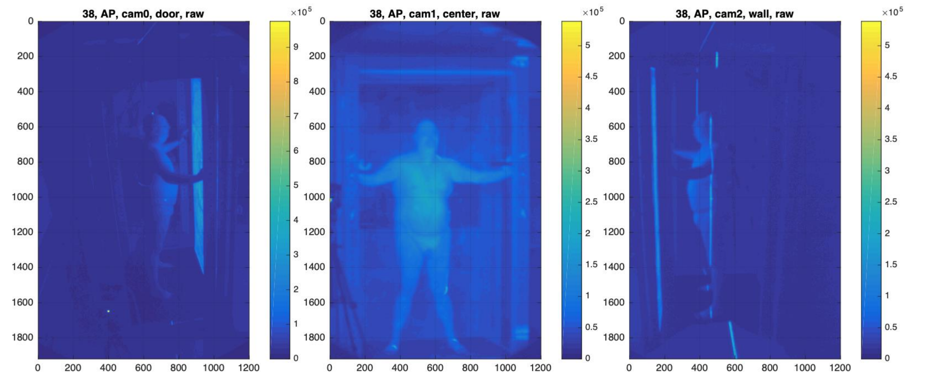

*Figure 7: Cherenkov images (door, center, and wall) of patient #38 for AP position using dual-field 6 MeV HDTSe beam in TSET position (500 cm SSD).*

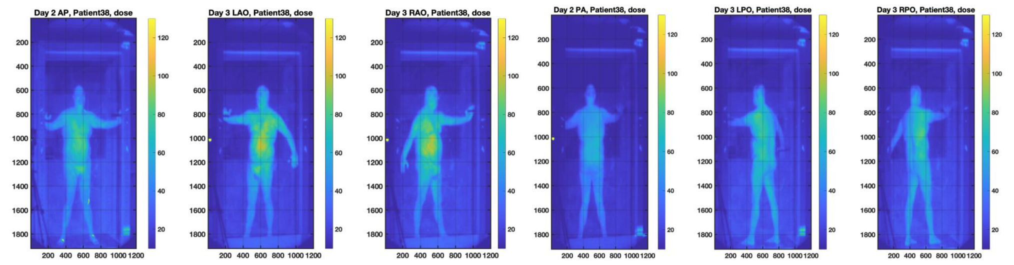

*Figure 8: Cherenkov-converted dose maps of patient #38 using dual-field 6 MeV HDTSe beams in the 6 TSET postures (500 cm SSD) from the center camera (cam1).*

## CONCLUSIONS

Using wall-mounted cameras provide improved reliability of daily camera positioning for application of flood fields to reduce uncertainty due to pixel-to-pixel sensor sensitivity variations.

The dose on the sides of the phantom are consistently lower than the dose facing the radiation and the dose ratios range from 0.24 for a cube to 0.40 for a cylinder, the later is closer to that from *in-vivo* patient measurements. The dose ratio obtained from using multiple cameras for patient side and for vertex is lower than the ratios of dose based on the front camera alone (see Fig. 8). We will use the patient postures based on 3D scans (Fig. 6) to perform MC simulations to validate the experimental findings.

More works are needed to fully calibrate the multiple-camera setup to determine correct dose accumulation on the patient body.

## REFERENCES

[1] Elsayad, K., et. al., "Total Skin Electron Beam Therapy as Part of Multimodal Treatment Strategies for Primary Cutaneous T-Cell Lymphoma," *Oncol Res and Treat, 40, 244-252* (2017).

[2] Yunhe Xie, Heather Petroccia, Amit Maity, Tianshun Miao, Yihua Zhu, Petr Bruza, Brian W. Pogue, John P. Plastaras, Lei Dong, and Timothy C. Zhu, "Cherenkov imaging for Total Skin Electron Therapy (TSET)," Med Phys 47(1): 201-212, (2020).

[3] R. S. Cox, R. J. Heck, P. Fessenden, C. J. Karzmark, and D. C. Rust, "Development of total-skin electron therapy at two energies," Int. J. Radiat. Oncol. Biol. Phys. 18, 659-669, 1990.

## ACKNOWLEDGEMENTS

We thank Dr. Michael Jermyn from DoseOptics, LLC for technical support. We thank David Farraday and kendra Poirier for clinical trial support. We thank Giovanna Sorber, Meghan Minner, and Dexter Wilson for TSET treatment and patient support. This research is supported by National institute of Health (NIH) grant R21 CA239127.

## CONTACT INFORMATION

Timothy.Zhu@pennmedicine.upenn.edu, 1(215)-662-4043.